*Int. J. Electrochem. Sci.*, 7 **(2012)** 4929 - 4941

International Journal of
ELECTROCHEMICAL
SCIENCE
www.electrochemsci.org

# Investigation of the Inhibiting Effect of Some Triazole Derivatives for the Corrosion of Mild Steel in 1 M $H_2SO_4$ Solution

*Y. H. Ahmad, A. S. Mogoda*[*], *A. G. Gadallh*

Chemistry Department, Faculty of Science, Cairo University, Giza-12613, Egypt
[*]E-mail: awad_mogoda@hotmail.com

*Received:* 18 March 2012 / *Accepted:* 12 May 2012 / *Published:* 1 June 2012

The corrosion inhibition of steel in 1.0 M $H_2SO_4$ by some triazole derivatives namely, 4-amino-1,2,4-triazole-3-thiol (ATT), 4-amino-5-methyl-1,2,4-triazole-3-thiol (AMTT) and 4-amino-5-ethyl-1,2,4-triazole-3-thiol (AETT) has been studied using potentiodynamic polarization, electrochemical impedance spectroscopy (EIS) and Scanning electron microscopy (SEM). The results revealed that the inhibition efficiency increases as the inhibitor concentration increases and follows the order (ATT< AMTT< AETT). The adsorption of the triazole derivatives onto the steel surface obeys Langmuir adsorption isotherm with small negative values of $\Delta G_{ads}$ (less than 20 kJ) which ensures the spontaneous physical adsorption process. The surface examination using scanning electron microscope confirms the extra ordinary efficiency of the used inhibitors in protection of steel from corrosion as indicated by electrochemical measurements.

**Keywords:** Mild steel; Corrosion; Triazole Derivatives; Impedance

## 1. INTRODUCTION

The study of corrosion of steel in acid solutions and its inhibition have practical importance. Acid solutions are widely used in different industrial processes, for example, in acid pickling, scale removal in metallurgy, acid cleaning in boilers and oil-well cleaning [1]. Sulfuric acid is used in the steel surface treatment due to its lower cost, minimal fumes and non-corrosive nature of the $SO_4^{2-}$ ion [2]. Most of the well-known acid inhibitors are organic compounds containing electronegative atoms (such as N, S, P and O), unsaturated bonds (double or triple bonds), and plane conjugated systems including all kinds of aromatic cycles [3-12]. The compounds containing both nitrogen and sulfur can provide excellent inhibition, compared with compounds containing only nitrogen or sulfur [13,14]. Organic compounds used as inhibitors act through a process of surface adsorption, so the efficiency of

an inhibitor depends on the chemical structure of the organic compound, the surface charge of the metal, and the type of interaction between the organic molecule and metal surface [15]. In the present study, the efficiency of the tested three triazole derivatives as corrosion inhibitors of mild steel in 1.0 M $H_2SO_4$ solution was investigated on the basis of potentiodynamic polarization and electrochemical impedance spectroscopy (EIS) measurements. The electrochemical measurements were confirmed using scanning electron microscopy (SEM).

## 2. EXPERIMENTAL

Steel rod of the following chemical composition (wt%) was used in the experiments: (wt %); 0.31 C, 0.21 Si, 0.81 Mn, 0.014 P, 0.017 S, 0.06 Cu, 0.02 Cr, 0.01 Mo, 0.02 Ni, 0.002 V and the balance is Fe.

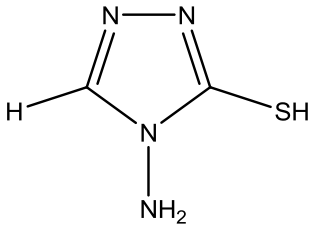


4-amino-1,2,4-triazole-3-thiol

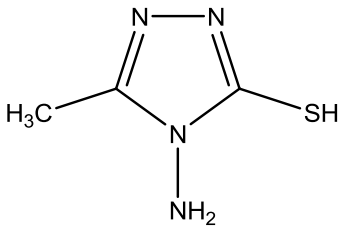


4-amino-5-methyl-1,2,4-triazole-3-thiol

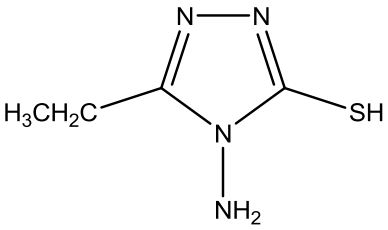


4-amino-5-ethyl-1,2,4-triazole-3-thiol

**Scheme 1.**

The rod was fixed into a glass tube with epoxy resin leaving a cross-sectional area of 0.50 $cm^2$ to contact the solution. Before immersion in the test solution, the electrode surface was mechanically polished using successively finer grade of emery papers (500-1200 grade), washed with double-distilled water, degreased in ethanol, and finally dried at room temperature. The acid solution was made from AR grade $H_2SO_4$ and double-distilled water. The molecular structures and names of the organic inhibitors are shown in Scheme 1.

A conventional three-electrode cell, which contained 100 ml of electrolyte solution, was used with a platinum sheet counter electrode, $Hg/Hg_2SO_4$ (in 1.0 M $H_2SO_4$ solution) as a reference electrode and steel rod as a working electrode. All the potentials reported to $Hg/Hg_2SO_4$. The electrochemical impedance spectroscopy (EIS) measurements were carried out using the electrochemical workstation IM6e Zahner-electrik GmbH, Meβtechnik, Kronach, Germany. The sinusoidal potential perturbation was 10 mV in amplitude over a frequency range of 0.1 Hz to 100 kHz. Polarization measurements were carried out at a scan rate of 1 mV $s^{-1}$ using EG&G (Princeton Applied Research) model 273A Potentiostat/Galvanostat interfaced to an IBM PS/3 computer. Before impedance or polarization measurements, the working electrode was immersed in the test solution until a steady-state of the open-circuit potential was reached. Scanning electron microscopy images were performed with Philips Quanta FEG microscope. The detail of the experimental procedures were described elsewhere [16,17].

## 3. RESULTS AND DISCUSSION

### *3.1. EIS measurements*

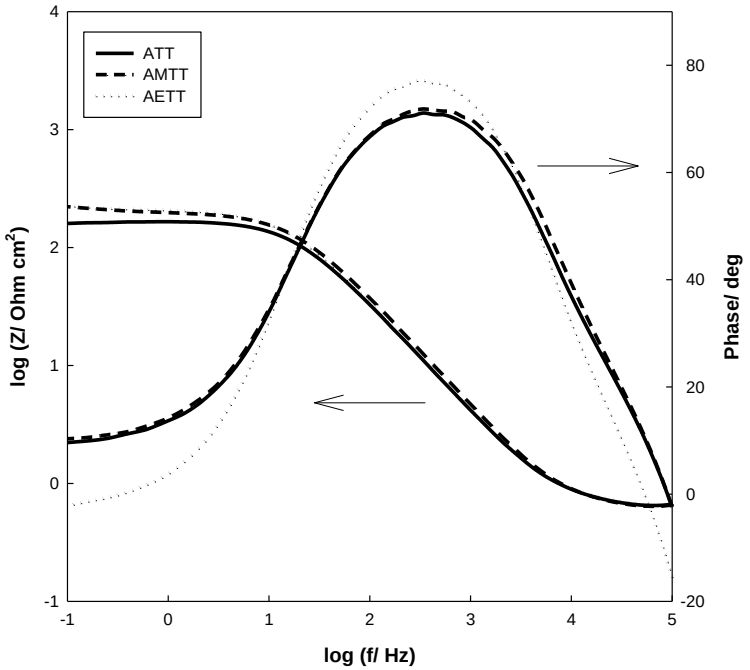


**Figure 1.** Bode impedance plots of mild steel in 1.0 M $H_2SO_4$ solution containing $1.0x10^{-3}$ M of ATT, AMTT and AETT.

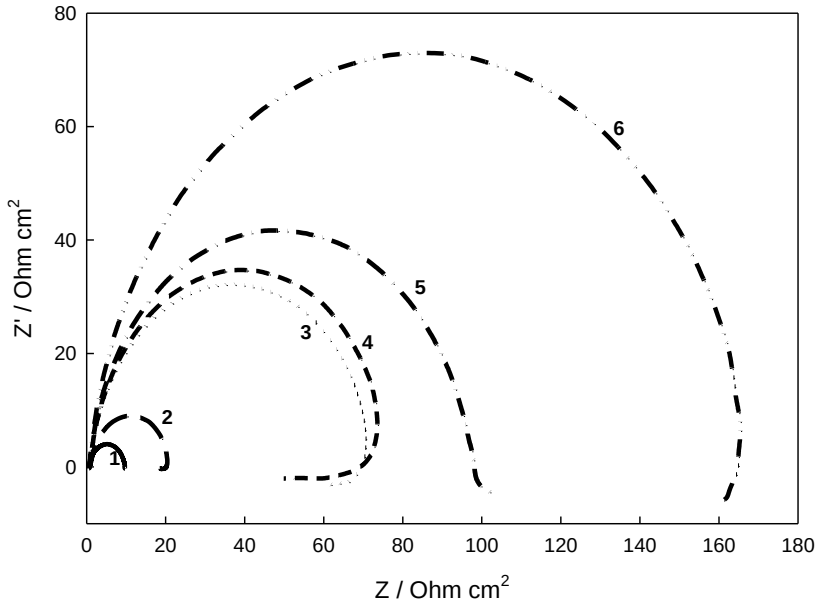


**Figure 2.** Nyquist impedance plots of mild steel in 1.0 M $H_2SO_4$ in absence and presence of different concentrations of ATT. blank (1), $1.0x10^{-4}$ M (2), $3.0x10^{-4}$ M (3), $5.0x10^{-4}$ M (4), $8.0x10^{-4}$ M (5) and $1.0x10^{-3}$ M (6)

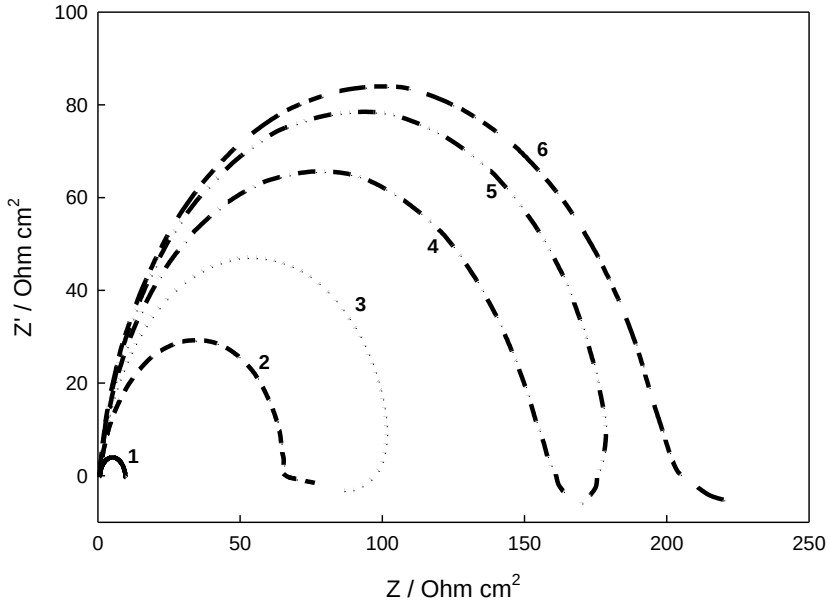


**Figure 3.** Nyquist impedance plots of mild steel in 1.0 M $H_2SO_4$ in absence and presence of different concentrations of AMTT. blank (1), $1.0x10^{-4}$ M (2), $3.0x10^{-4}$ M (3), $5.0x10^{-4}$ M (4), $8.0x10^{-4}$ M (5) and $1.0x10^{-3}$ M (6)

Bode and Nyquist plots of steel in 1.0 M $H_2SO_4$ solution in absence and presence of various concentrations of the tested triazole derivatives are given in Figs. 1-4. From Bode plot format we can easily identify the frequency break points associated with each limiting step and provides information

on the respective rates or relaxation times. It is clear from Fig. 1 that the process occurring on the steel surface is controlled by two time constants and the relaxation times of the two limiting steps are independent on the nature of the inhibitor used. Also, the impedance value |Z| increases in the order AETT > AMTT > ATT. The increase of |Z| can be attributed to the formation of a passive layer on the steel surface.

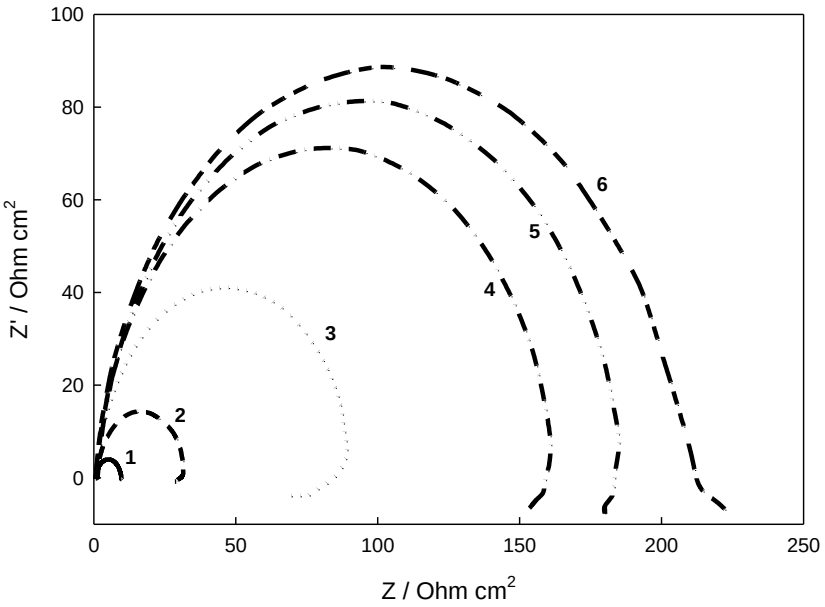


**Figure 4.** Nyquist impedance plots of mild steel in 1.0 M $H_2SO_4$ in absence and presence of different concentrations of AETT. blank (1), $1.0x10^{-4}$ M (2), $3.0x10^{-4}$ M (3), $5.0x10^{-4}$ M (4), $8.0x10^{-4}$ M (5) and $1.0x10^{-3}$ M (6)

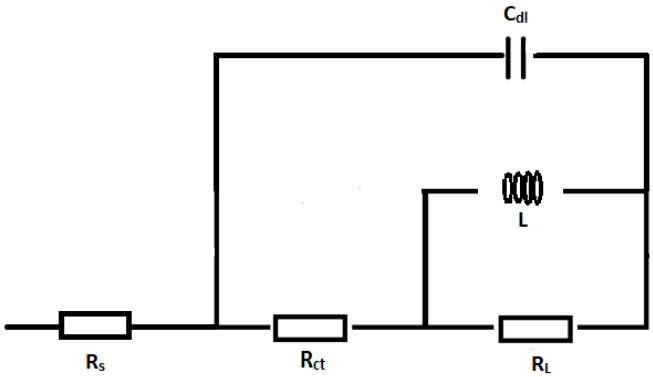


**Figure 5.** The equivalent circuit model used to fit the impedance spectra measured for mild steel in different solutions.

The Nyquist plots in Figs 2-4 are not perfect semicircles as expected from the theory of EIS. The deviation from ideal semicircle is generally attributed to the frequency depression as well as to the inhomogeneities of electrode surface and mass transport resistance [18]. The diameter of the

impedance semicircles increased after the addition of inhibitors to the aggressive corrosive medium (1.0 M $H_2SO_4$). This increase is more pronounced as the concentration of inhibitor increases which indicates adsorption of inhibitor molecules onto the metal surface [18]. The impedance data were analyzed using software provided with the electrochemical workstation and fitted to the equivalent circuit model shown in Fig 5, with mean error in impedance of 1% and mean error in phase 0.3%. The appropriate equivalent model includes a solution resistance, $R_s$, a double layer capacitance, $C_{dl}$, and a charge transfer resistance, $R_{ct}$. The second parallel combination of L and $R_L$ was introduced to account for the inductive loop observed in The Nyquist diagrams. The presence of this low frequency inductive loop may be attributed to the relaxation process obtained by adsorption of species $(SO_4^{2-})_{ads}$ and $(H^+)_{ads}$ on the electrode surface. It may also be attributed to the re-dissolution of the passivated surface [19,20].

In case of the electrochemical impedance spectroscopy, the inhibition efficiency ($\eta_I$ %) was calculated using charge transfer resistance according to the following equation [10]:

$$\eta_I\% = \frac{R_{ct} - R^0_{ct}}{R_{ct}} x100 \qquad (1)$$

Where $R^0_{ct}$ and $R_{ct}$ are the charge transfer resistance values in absence and presence of inhibitor, respectively. The equivalent circuit parameters and the inhibition efficiency $\eta_I$ % are listed in Table 1.

**Table 1.** The equivalent circuit parameters obtained from fitting of impedance data measured for mild steel in different solutions to the theoretical model.

| Inhibitor Type | Inhibitor Concentration/ mol $L^{-1}$ | $R_S$/ Ohm $cm^2$ | L/ Henry $cm^2$ | $R_l$/ Ohm $cm^2$ | $C_{dl}$/ $\mu F\ cm^{-2}$ | $\alpha$ | $R_{ct}$/ Ohm $cm^2$ | Inhibition efficiency $\eta_I$/ % |
|---|---|---|---|---|---|---|---|---|
| Blank (1.0 M $H_2SO_4$) | | 0.68 | 1.389 | 0.720 | 304.0 | 0.925 | 8.275 | - |
| ATT | $1.0 \times 10^{-4}$ | 0.755 | 1.461 | 2.610 | 111.7 | 0.870 | 18.04 | 54.10 |
| | $3.0 \times 10^{-4}$ | 0.747 | 1.489 | 10.68 | 53.18 | 0.916 | 64.70 | 87.20 |
| | $5.0 \times 10^{-4}$ | 0.771 | 1.484 | 7.985 | 62.42 | 0.911 | 64.85 | 87.23 |
| | $8.0 \times 10^{-4}$ | 0.739 | 1.477 | 4.514 | 52.16 | 0.919 | 92.75 | 91.07 |
| | $1.0 \times 10^{-3}$ | 0.694 | 1.478 | 5.685 | 39.9 | 0.927 | 159.75 | 94.82 |
| AMTT | $1.0 \times 10^{-4}$ | 0.695 | 1.409 | 1.192 | 47.86 | 0.902 | 66.25 | 87.50 |
| | $3.0 \times 10^{-4}$ | 0.691 | 1.412 | 1.412 | 46.12 | 0.915 | 95.70 | 91.35 |
| | $5.0 \times 10^{-4}$ | 0.706 | 1.410 | 2.169 | 39.52 | 0.923 | 151.25 | 94.53 |
| | $8.0 \times 10^{-4}$ | 0.685 | 1.433 | 5.475 | 37.20 | 0.929 | 172.4 | 95.20 |
| | $1.0 \times 10^{-3}$ | 0.681 | 1.410 | 2.662 | 35.50 | 0.931 | 193.25 | 95.72 |
| AETT | $1.0 \times 10^{-4}$ | 0.765 | 1.460 | 4.307 | 86.40 | 0.896 | 70.80 | 88.31 |
| | $3.0 \times 10^{-4}$ | 0.706 | 1.474 | 9.905 | 50.76 | 0.914 | 98.50 | 91.55 |
| | $5.0 \times 10^{-4}$ | 0.755 | 1.460 | 4.668 | 41.14 | 0.929 | 155.7 | 94.68 |
| | $8.0 \times 10^{-4}$ | 1.316 | 1.459 | 4.604 | 37.46 | 0.927 | 179.3 | 95.38 |
| | $1.0 \times 10^{-3}$ | 0.714 | 1.454 | 3.565 | 39.28 | 0.930 | 201.65 | 95.89 |

It can be seen from the results that, the charge transfer resistance ($R_{ct}$) increases as the inhibitor concentration increases. The increase in $R_{ct}$ values is attributed to the formation of protective film on the electrode surface whose thickness increases with increasing the inhibitor concentration [21]. Also, the capacitance of the electric double layer ($C_{dl}$) decreases in the presence of inhibitors due to a decrease in local dielectric constant and/or increase in the thickness of the double layer [22]. According to these results the triazole derivatives tested here inhibit the iron corrosion by adsorption at steel/solution interface. The lower values of $C_{dl}$ may be a result of replacement of water molecules by inhibitor molecules at the electrode surface through adsorption:

$$Org_{(sol)} + nH_2O_{(ads)} \longrightarrow Org_{(ads)} + nH_2O_{(sol)} \qquad (2)$$

where $Org_{(sol)}$ and $Org_{(ads)}$ are the organic molecules in the solution and adsorbed on the metal surface, respectively, and n is the number of water molecules replaced by the organic molecules [18]. From Table 1 it is clear that the inhibition efficiency $\eta_I$ increases with increase of the inhibitor concentration and the values of $\eta_I$ follow the order: ATT < AMTT < AETT. This means that as the side chain length of the inhibitor molecule increases, the surface coverage increases which leads to an increase in $\eta_I$.

*3.2. Potentiodynamic polarization*

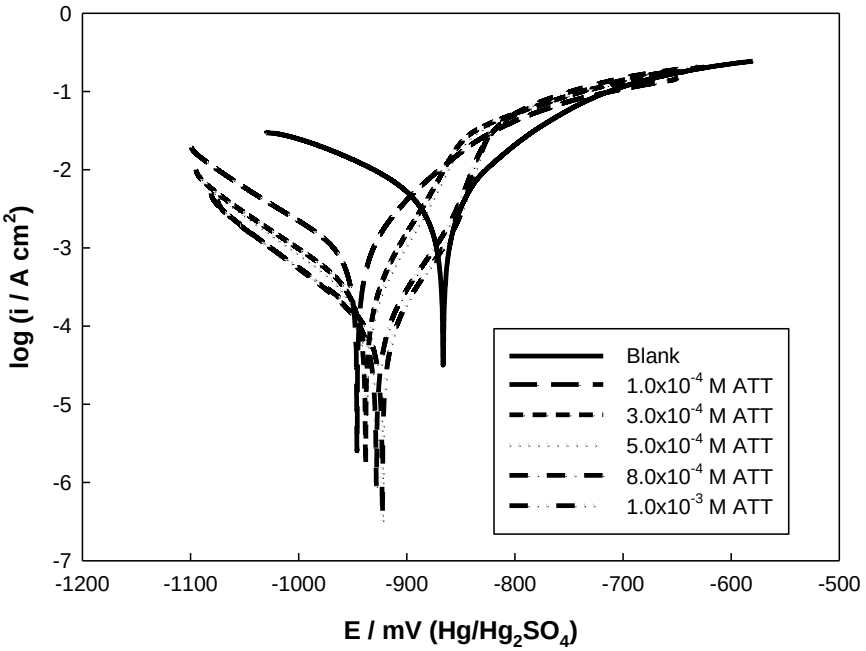


**Figure 6.** The potentiodynamic polarization curves of mild steel in 1.0 M $H_2SO_4$ in absence and presence of different concentrations of ATT.

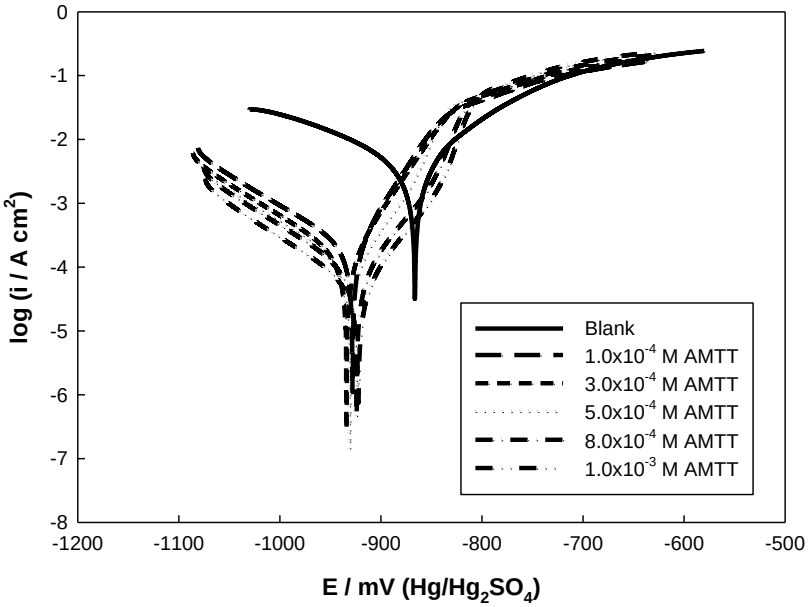


**Figure 7.** The potentiodynamic polarization curves of mild steel in 1.0 M $H_2SO_4$ in absence and presence of different concentrations of AMTT.

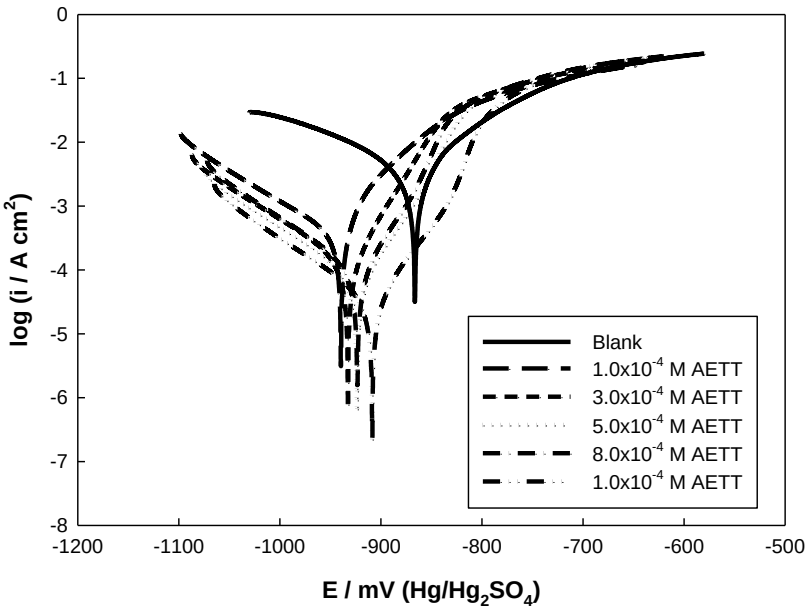


**Figure 8.** The potentiodynamic polarization curves of mild steel in 1.0 M $H_2SO_4$ in absence and presence of different concentrations of AETT.

Potentiodynamic polarization curves of steel in 1.0 M $H_2SO_4$ in the absence and presence of various concentrations of the three triazole derivatives are shown in Figs. 6-8. It is clear from figures that both anodic and cathodic reactions of steel corrosion were suppressed in the presence of inhibitors,

and the suppression effect increases with the increase of the concentration of these inhibitors. The electrochemical parameters, corrosion potential ($E_{corr}$), cathodic and anodic Tafel slopes ($\beta_c$ and $\beta_a$) and corrosion current density ($i_{corr}$), obtained by extrapolation of Tafel lines, are presented in Table 2.

**Table 2.** The corrosion parameters for mild steel in 1.0 M $H_2SO_4$ in absence and presence of different concentrations of triazole derivatives

| Inhibitor type | Inhibitor concentration / mol $L^{-1}$ | $E_{Corr}$ / mV $Hg/Hg_2SO_4$ | $i_{Corr}$ / $\mu A\ cm^{-2}$ | βa / mV $decade^{-1}$ | βc / mV $decade^{-1}$ | Corrosion rate / mpy | Inhibition efficiency $\eta_p$/ (%) |
|---|---|---|---|---|---|---|---|
| Blank (1 M $H_2SO_4$) | | - 867.2 | 4.95 x$10^3$ | 226.5 | 186.4 | 2.272 x $10^3$ | - |
| ATT | 1.0 x 10-4 | - 947.3 | 578.4 | 197.9 | 102.5 | 265.1 | 88.33 |
| | 3.0 x 10-4 | - 939.8 | 189.8 | 227.5 | 94.38 | 87.00 | 96.17 |
| | 5.0 x 10-4 | - 939.4 | 159.5 | 220.4 | 92.34 | 72.54 | 96.78 |
| | 8.0 x 10-4 | - 929.3 | 73.54 | 191.3 | 86.61 | 33.71 | 98.52 |
| | 1.0 x 10-3 | - 923.7 | 71.22 | 218.1 | 90.12 | 32.64 | 98.56 |
| AMTT | 1.0 x 10-4 | - 930.2 | 137.7 | 217.4 | 91.35 | 63.15 | 97.22 |
| | 3.0 x 10-4 | - 935.7 | 104.2 | 204.7 | 89.11 | 47.74 | 97.90 |
| | 5.0 x 10-4 | - 932.2 | 74.38 | 215.9 | 87.39 | 34.10 | 98.50 |
| | 8.0 x 10-4 | - 925.2 | 54.24 | 188.3 | 86.74 | 24.86 | 98.91 |
| | 1.0 x 10-3 | - 923.5 | 30.30 | 163.0 | 83.00 | 13.89 | 99.39 |
| AETT | 1.0 x 10-4 | - 942.7 | 228.5 | 198.0 | 90.54 | 104.8 | 95.39 |
| | 3.0 x 10-4 | - 934.4 | 96.66 | 217.2 | 88.16 | 44.30 | 98.05 |
| | 5.0 x 10-4 | - 924.9 | 70.48 | 195.8 | 84.87 | 32.30 | 98.58 |
| | 8.0 x 10-4 | - 924.6 | 52.19 | 206.8 | 82.86 | 23.92 | 98.95 |
| | 1.0 x 10-3 | - 909.7 | 22.32 | 143.3 | 81.54 | 10.23 | 99.55 |

The inhibition efficiencies $\eta_p$ % of the organic inhibitors at different concentrations in 1.0 M $H_2SO_4$ are also given in Table 2. The inhibition efficiency, $\eta_p$ % was calculated according to the relation [23]:

$$\eta_p\% = \frac{i^0_{corr} - i_{corr}}{i^0_{corr}} x100 \qquad (3)$$

Where $i^0_{corr}$ and $i_{corr}$ are the corrosion current densities in the absence and presence of inhibitor, respectively.

In acidic medium, the anodic reaction of corrosion is the passage of metal ions from the surface into the soln, and the cathodic reaction is the discharge of hydrogen ions to produce hydrogen gas or reduction of oxygen. The inhibitor may affect either the anodic or the cathodic reaction, or both [24,25]. The values of the anodic and cathodic Tafel slopes ($\beta_a$ and $\beta_c$) calculated for inhibited solutions are smaller than obtained for the uninhibited $H_2SO_4$ soln (see Table 2). This indicates that the inhibitor affected both the anodic and cathodic reactions of steel corrosion. Therefore, the studied inhibitors are mixed-type inhibitors. As can be seen from Table 2, the inhibition efficiency $\eta_p$ increases with increasing the inhibitor concentration and $\eta_p$ follows the order: ATT < AMTT < AETT.

Therefore, the inhibition efficiencies calculated from potentiodynamic polarization measurements show a similar trend as those obtained from impedance measurements.

### *3.3. Adsorption isotherm*

Adsorption isotherm can give important information about the interaction between the inhibitor and the metal surface [26]. The degree of surface coverage (θ) was calculated from the polarization measurements according to the following equation:

$$\theta = 1 - \frac{i_{corr}}{i_{corr}^{0}} \quad (4)$$

The plots of $C_{inh}/\theta$ against $C_{inh}$ for the three studied Triazole compounds give straight lines with almost unity slope (Fig 9), indicating that these inhibitors obey Langmuir adsorption isotherm which can be expressed as follows [27]:

$$\frac{C_{inh}}{\theta} = \frac{1}{K_{ads}} + C_{inh} \quad (5)$$

Where $C_{inh}$ is the inhibitor concentration and $K_{ads}$ is the equilibrium constant of the adsorption process. The $K_{ads}$ value may be taken as a measure of the strength of the adsorption forces between the inhibitor molecules and the metal surface [28].

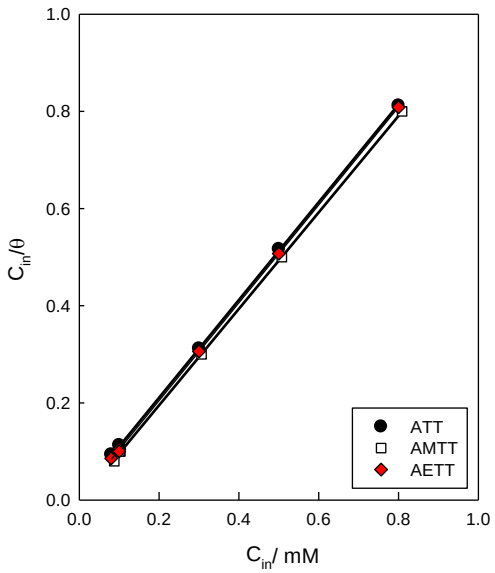


**Figure 9.** Langmuir adsorption isotherms of mild steel in 1.0 M $H_2SO_4$ containing different concentrations of triazole derivatives.

The adsorption constant, $K_{ads}$ is related to the standard free energy of adsorption, $\Delta G^0_{ads}$ by the following equation [29]:

$$\Delta G^0_{ads} = -RT\ln(55.5K_{ads}) \quad (6)$$

The value of 55.5 is the molar concentration of water in the solution expressed in mol $L^{-1}$. The values of $\Delta G^0_{ads}$ were found to be in the range of -21.09 to -23.73 kJ $mol^{-1}$ for the three tested inhibitors. As the value of $\Delta G^0_{ads}$ is more negative this reveals that the adsorption process on the metal surface takes place spontaneously and the adsorbed layer is more stable [30]. Generally, the values of $\Delta G^0_{ads}$ in the order of 20 kJ $mol^{-1}$ or less indicate physisorption, while those of the order of 40 kJ $mol^{-1}$ or higher involve charge sharing or charge transfer from the inhibitor molecules to the metal surface to form a coordinate type of bond (chemisorption) [31,32]. Therefore, the values obtained for $\Delta G^0_{ads}$ of the tested inhibitors on steel in 1.0 M $H_2SO_4$ confirms that adsorption is typical physisorption [33].

*3.4. SEM investigation*

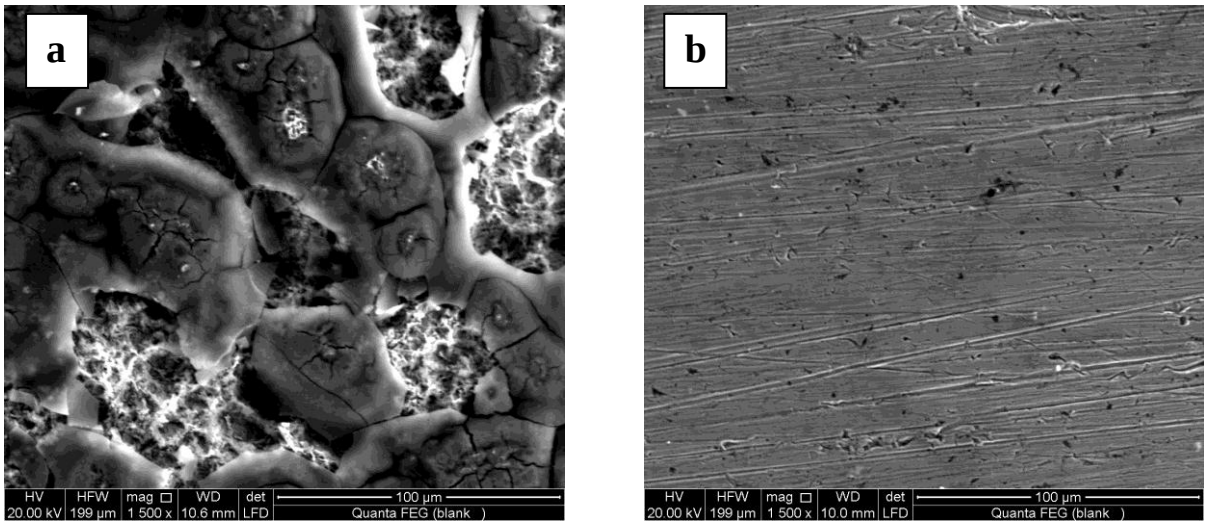


**Figure 10.** SEM micrographs of mild steel after 2h immersion in 1.0 M $H_2SO_4$ solution (blank) (a) and in 1.0 M $H_2SO_4$ solution containing $1.0x10^{-3}$ M AETT (b)

The inhibiting action of triazole compounds was confirmed by SEM. Fig 10a shows the scanning electron micrograph of the mechanically polished steel surface after immersion in 1.0 M $H_2SO_4$ for 2 h. The scanning micrograph of polished surface after immersion in 1.0 M $H_2SO_4$ solution containing $1x10^{-3}$ M AETT for the same time interval is presented in Fig 10b. It is clear that the presence of the organic inhibitor in the acid medium leads to a decrease in the defects and notches which are formed on the steel surface in absence of the inhibitor. Also, the inhibitor forms a layer of closely packed film onto the steel surface which explains the large decrease in the corrosion rate and the high inhibition efficiency.

## 4. CONCLUSIONS

- Triazole compounds studied are highly efficient inhibitors for both anodic and cathodic reaction by adsorption on the steel surface in 1.0 M $H_2SO_4$ solution.
- The inhibition efficiency increases by increasing the inhibitor concentration and follows the order: ATT < AMTT < AETT.
- The polarization measurements revealed that the used inhibitors are mixed-type inhibitors.
- The adsorption of the inhibitors on steel surface obeys Langmuir isotherm and represents a physical adsorption.

## References

1. V. S. Sastri, Corrosion Inhibitors-Principle and Applications, Wiley, Chichester, England, 1998.
2. R. Hasanov, S. Bilge, S. Bilgic, G. Gece, Z. Kilic, *Corros. Sci*., 52 (2010) 984.
3. J. Aljourani, K. Raeissi, M. A. Golozar, *Corros. Sci*., 51 (2009) 1836.
4. K. C. Emregül, O. Atakol, *Mater. Chem. Phys*., 82 (2003) 188.
5. A. Asan, M. Kabasakaloglu, M. Is Kalan, Z. Kilic, *Corros. Sci*., 47 (2005) 1534.
6. K. Stanly Jacob, G. Parameswaran, *Corros. Sci*., 52 (2010) 224.
7. Y. Tang, X. Yang, W. Yang, Y. Chen, R. Wana, *Corros. Sci*., 52 (2010) 242.
8. P. Lowmunkhong, D. Ungthararak, P. Sutthivaiyakit, *Corros. Sci*., 52 (2010) 30.
9. M. Abdallah, *Corros. Sci*., 44 (2002) 717.
10. M. A. Hegazy, *Corros. Sci*., 51 (2009) 2610.
11. A. Chetouani, A. Aouniti, B. Hammouti, N. Benchat, T. Benhadda, S. Kertit, *Corros. Sci*., 45 (2003) 1675.
12. A. Lgamri, H. Abou El-Makarim, A. Guebour, A. Ben Bachir, L. Aries, S. El-Hajjaji, *Progr. Org. Coat.*, 48 (2003) 63.
13. J. Aljourani, M. A. Golozar, K. Raesis, *Mater. Chem. Phys*., 121 (2010) 320.
14. Y. Abboud, A. Abourriche, T. Saffaj, M. Berrada, M. Charrouf, A. Bennamara, N. Al Himidi, H. Hannache, *Mater. Chem. Phys*., 105 (2007) 1.
15. Ü. Ergun, D. Yüzer, K. C. Emregül, *Mater. Chem. Phys*., 109 (2008) 492.
16. A. S. Mogoda, Y. H. Ahmad, W. A. Badawy, *J. Appl. Electrochem*., 34 (2004) 873.
17. A. S. Mogoda, Y. H. Ahmad, W. A. Badawy, *Mater. Chem. Phys*., 126 (2011) 676.
18. R. Solmaz, *Corros. Sci*., 52 (2010) 3321.
19. H. H. Hassan, *Electrochim. Acta*, 53 (2007) 1722.
20. H. H. Hassan, E. Abdelghani, M. A. Amin, *Electrochim. Acta*, 52 (2007) 6359.
21. S. K. Shukla, M. A. Quraish, *Mater. Chem. Phys*., 120 (2010) 142.
22. M. Behpour, S. M. Ghoreishi, N. Soltani, M. Salavati-Niasari, *Corros. Sci*., 51 (2009) 1073.
23. El-Mehdi, B. Mernari, M. Traisnael, F. Bentiss, M. Lagrenee, *Mater. Chem. Phys*., 77 (2002) 489.
24. S. V. Ramesh, A. V. Adhikari, Corros. Sci., 50 (2008) 55.
25. A. Y. Musa, A. A. H. Kadhum, A. B. Mohamad, M. S. Takriff, A. R. Daud, S. K. Kamarudin, *Corros. Sci.*, 52 (2010) 526.
26. K. C. Emregul, E. Duzgun, O. Atakol, *Corros. Sci*., 48 (2006) 3243.
27. O. K. Abiola, J. O. E. Otaigbe, *Corros. Sci*., 51 (2009) 2790.
28. M. A. Amin, *J. Appl. Electrochim*., 36 (2006) 215.
29. N. V. Likhanova, M. A. Domnguez-Aguilar, O. Olivares-Xometl, N. Nava-Entzana, E. Arce, H. Dorantes, *Corros. Sci*., 52 (2010) 2088.

30. M. Scendo, M. Hepel, *J. Electroanal. Chem*., 613 (2008) 35.
31. F. M. Donahue, K. Nobe, *J. Electrochem. Soc*., 112 (1965) 886.
32. K. F. Khaled, N. Hackerman, *Electrochim. Acta*, 49 (2004) 485.
33. F. El-Taib Heakal, A. M. Fekry, *J. Electrochem. Soc*., 155 (2008) C 534.